Project and Site Condition

The overall project was a comprehensive revitalization of the river navigation facilities on the lower Monogahela River. The project involved the construction of a new gated dam to replace the over 100-year old existing No. 2 dam, which has displayed serious structural deficiencies. During the design phase of the caissons supporting the dam, AWK Consulting Engineers, Inc. conducted a fully instrumented field test assisted by its sub-consultant, Lyman C. Reese and Assoc. Portions of the field test data were used for analysis and preparation of this paper.

The river bottom at the test site was composed of a 4.4-m (14.5-ft) thick layer of alluvium followed successively by a 3.2-m (10.5-ft) layer of clayshale/claystone, a 7.9-m (26-ft) layer of weathered siltstone, and a thick stratum of siltstone. The alluvium was classified as SP-SC and had a submerged unit weight of 9.8kN/m^3 (62.2 pcf) with an internal friction angle of 34 degrees. The properties of underlying rock are summarized in Table 1 below.

Table 1. Rock Properties

Soil/Rock Layer	Unit Weight (kN/m^3/pcf)	Elastic Modulus (kPa/psi)	Cohesion (kPa/psi)
Clayshale/Claystone	15.5/98.5	7.5x10^5/1.1x10^5	2.1x10^3/306
Weathered Siltstone	16.0/102	1.8x10^6/2.6x10^5	11.6x10^3/1,694
Siltstone	16.0/102	3.0x10^6/4.3x10^5	16.9x10^3/2,458

Caisson Instrumentation and Testing

Two 1.5-m (5-ft) diameter reinforced concrete caissons were tested. Their lengths were 9.4 m (31 ft) for caisson A (upstream) and 12.5 m (41 ft) for caisson B (downstream). The two caissons were approximately 15.2 m (50 ft) apart, and were reinforced with 12 #18 primary and #8 spiral rebars. The caissons were socketed in the rock stratum to a depth of about 4.6m (15-ft) for caisson A and 7.6 m (25 ft) for caisson B. They were instrumented with vibrating wire strain gages along the loading axis for measuring concrete and rebar strains, inclinometers installed inside the caisson for monitoring caisson deflection, and electrolytic tilt sensors installed at the head for monitoring caisson head rotation.

The test loading was applied by pulling the two caissons together via a high strength steel tension bar located approximately 0.3 m (1 ft) above the dredge line. A 305-mm (12-in) stroke center-hole hydraulic jack mounted on the steel tension bar at the downstream side of caisson B was used for pulling. The standard test procedures of ASTM D-3966 on testing piles under lateral load were followed. The maximum test load applied was based on the assumed lateral load capacity of 779 kN (175 kips). The test data were recorded for each level of loading at different durations using a data logging system. An elevation view of the test set-up with instrumentation is depicted in Figure 1. The details on caisson construction, instrumentation, and testing are available elsewhere (Hall, 1999).

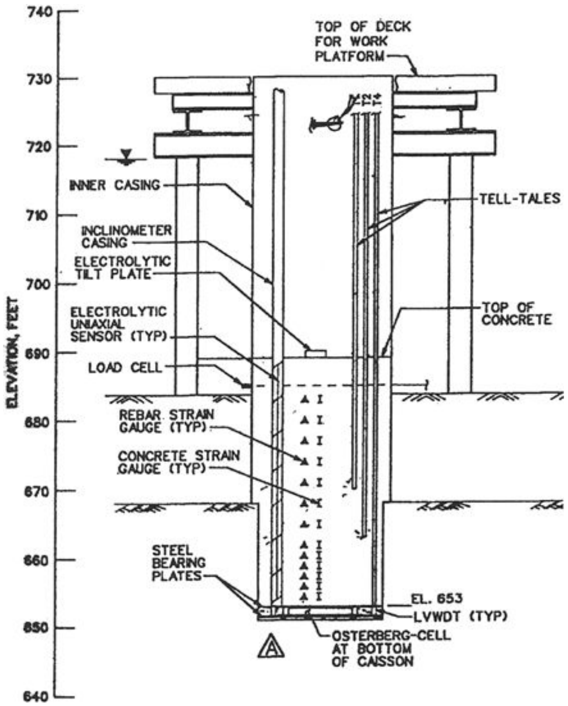

Figure 1. Test Caisson A Elevation View with Instrumentation

Field Data Analysis

The field data were analyzed following the procedures of Matlock and Ripperger (1956). The analysis began with the determination of bending moment profiles from the measured strain data. The bending moment profiles were then used to obtain deflection profiles through double integrations, and soil reaction profiles through double differentiations of the bending moment profiles.

Deflection is a function of bending stiffness and bending moment. Because cracking in the reinforced concrete member influences bending stiffness, bending stiffness is also a function of bending moment. Therefore, the relationship between bending stiffness and bending moment is needed in the analysis of deflection profile.

The bending stiffness vs. bending moment relations were first analyzed by means of computer analysis using Ensoft LPILE, which was an upgraded Windows based version of the Ensoft COM624 program. Input data was based on widely used reinforced concrete properties and design dimensions of test caisson A. The relationship obtained was then used to determine caisson deflections. The computed deflections were considerably smaller than the measured values. The discrepancy can be attributed primarily to the input reinforced concrete properties which may not be representative of the field condition. To obtain more accurate deflection profiles, the bending stiffness vs. bending moment relation was then analyzed using the measured strain data. The re-computed deflection profiles agreed with the measured data fairly well.

The soil/rock reaction profiles for various load intensities were analyzed by performing double differentiations of the bending moment profiles. Knowing the soil/rock reaction (*p*) and the corresponding lateral deflection (*y*) for various loading intensities, experimental *p-y* curves were determined at various points along the rock socket. Because sufficient deflection data were not available for the lower portion of the rock socket, the experimental *p-y* curves were analyzed only for the top 3.2-m (10.5-ft) of the clayshale layer. This clayshale layer was highly to moderately fractured. More specifically, the upper portion of the clayshale layer was soft, broken to highly fractured, slickensided with soil filled joints, spaced at less than 60 mm (2.4 in); the lower portion was moderately hard, highly to moderately fractured, smooth sided with closed joints, spaced at 60 to 200 mm (2.4-7.9 in).

Theoretical Analysis and Comparison

To take into consideration the varying rock mass condition across the clayshale layer, the entire layer was divided into three sublayers: 1.1 m (3.5 ft) at top, 0.6 m (2.0 ft) in the middle, and 1.5 m (5.0 ft) at bottom. For each sublayer, the upper and lower bound values of RQD (rock quality designation), E_L (laboratory modulus), MRR (modulus reduction ratio), E_{mass} (rock mass modulus), and q_u (uniaxial compressive strength) were obtained. Because of the variability in rock quality laterally as well as vertically, the RQD values were obtained from borings located at or very close to the test shaft location. The values of MRR were estimated from the MRR vs. RQD correlation proposed by Bieniawski (1978). The values of E_{mass} were computed from MRR multiplied by E_L. All of these data are tabulated in Table 2.

The values of E_{mass} were also evaluated using RMR (rock mass rating) correlation of Halcrow (1993). The upper and lower bound values of RMR, the associated parameters, and the evaluated E_{mass} are shown in Table 3. Using the material properties obtained independently from RQD and RMR correlations, theoretical *p-y* curves for caisson A were determined using the procedures proposed by Reese (1997). Note that due to unavailability of complete field test data for caisson B, only the *p-y* curves of caisson A were analyzed in Figures 2(a,b) and 3(a,b). These *p-y* curves were compared with those derived from the test data of caisson A. The comparison showed that the *p-y* curves obtained from RMR correlation were more reasonable than those from RQD correlation because they were bracketed between upper and lower bound curves. The curves obtained from RQD were less consistent with the experimental *p-y* curves and in most cases produced high and low bound bracket curves much different than the experimental curves.

Table 2. Input Rock Properties Obtained from the RQD Correlation

	RQD (%)	E_L (kPa /psi)	MRR	E_{mass} (kPa /psi)	q_u (kPa /psi)
Upper Clayshale Layer					
Upper Bound	20	$4.1x10^5/.06x10^6$	.10	$4.1x10^4/6.0x10^3$	$4.1x10^3/0.6x10^3$
Lower Bound	35	$5.2x10^5/.075x10^6$	.15	$6.6x10^4/9.6x10^3$	$5.5x10^3/0.8x10^3$
Middle Clayshale Layer					
Upper Bound	40	$6.9x10^5/.10x10^6$	.17	$1.2x10^5/1.7x10^4$	$7.6x10^3/1.1x10^3$
Lower Bound	50	$8.9x10^5/.13x10^6$	.20	$1.5x10^5/2.2x10^4$	$9.0x10^3/1.3x10^3$
Lower Clayshale Layer					
Upper Bound	70	$1.2x10^6/.18x10^6$	.33	$4.1x10^5/6.0x10^4$	$1.0x10^4/1.5x10^3$
Lower Bound	100	$1.4x10^6/.21x10^6$	.80	$1.1x10^6/1.6x10^5$	$1.4x10^4/2.0x10^3$

Note: RQD (Rock Quality Designation)
E_L (Elastic Modulus of Laboratory Sample)
MRR (Modulus Reduction Ratio)
E_{mass} (Elastic Modulus of Rock Mass
q_u (Unconfined Compression Strength)

Table 3. Input Rock Properties Obtained from RMR Correlations

Upper Clayshale Layer	Input Value/Rating	Input Value/Rating
RMR Evaluation Parameters	Lower Bound	Upper Bound
Unconfined Compressive Strength, kPa/ psi	4,134(600)/1	5,512(800)/1
RQD(%)	20/3	35/5
Discontinuity Spacing (mm)	<60/5	<60/5
Conditions of Discontinuities	Gouge>5mm/0	Gouge>5mm/0
Ground Water (General Conditions)	Dripping/4	Dripping/4
RMR Value	12	15
E_{mass} (kPa/psi)	21,000/3,000	48,000/7,000
Middle Clayshale Layer		
Unconfined Compressive Strength, kPa/psi	5,512 (800)/1	8,957(1,300)/2
RQD(%)	40/7	50/8
Discontinuity Spacing (mm)	<60/5	<60/5
Conditions of Discontinuities	Gouge>5mm/0	Gouge<5mm/5
Ground Water (General Conditions)	Dripping/4	Dripping/4
RMR Value	17	27
E_{mass} (kPa/psi)	82,000/12,000	330,000/48,000
Lower Clayshale Layer		
Unconfined Compressive Strength, kPa/psi	10,335(1,500)/2	13,780 (2000)/2
RQD(%)	70/14	100/8
Discontinuity Spacing (mm)	60-200/7	6-200/7
Conditions of Discontinuities	Gouge<5mm/5	Moderate Weathering/6
Ground Water (General Conditions)	Dripping/4	Dripping/6
RMR Value	32	37
E_{mass} (kPa/psi)	$1.0x10^6/1.5x10^5$	$1.7x10^6/2.5x10^5$

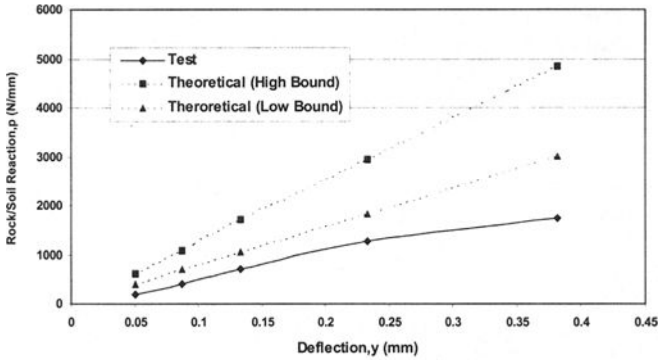

Figure 2 (a). ***p-y*** **Curves Obtained from RQD Correlation (Upper Layer)**

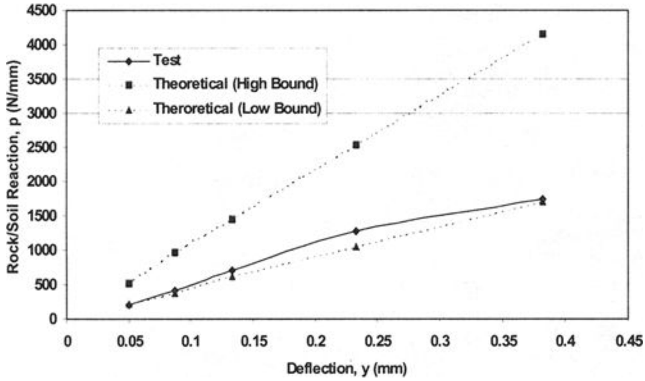

Figure 2 (b). ***p-y*** **Curves Obtained from RMR Correlation (Upper Layer)**

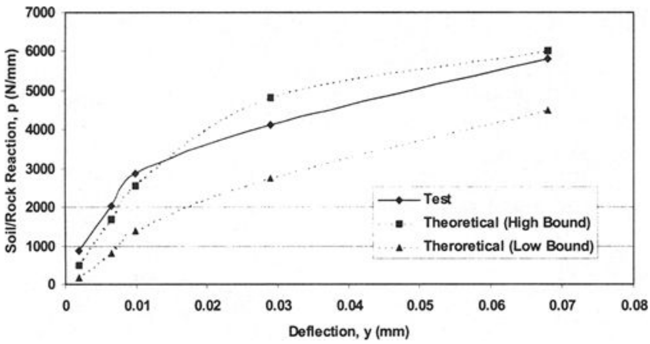

Figure 3 (a). ***p-y*** **Curves Obtained from RQD Correlation (Upper Layer)**

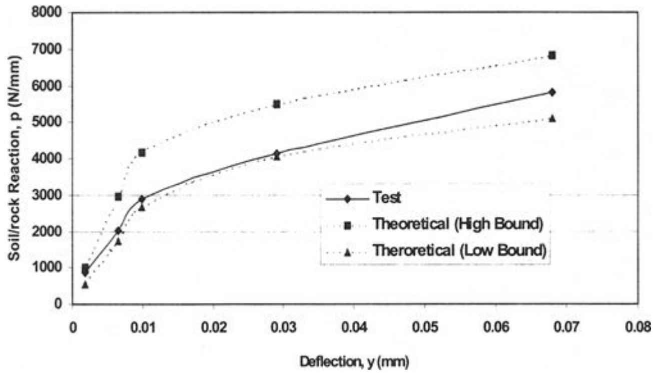

Figure 3 (b). ***p-y*** **Curves Obtained from RMR Correlation (Lower Layer)**

The in-situ properties of clayshale were back-calculated by fitting the theoretical *p-y* curves to the *p-y* curves obtained from the strain data of caisson A. The curve fitting was performed in two steps. The first step employed an iterative process whereby the values of compressive strength and elastic modulus within the prescribed upper and lower bounds were varied to produce the best-fit curve for each clayshale sub-layer. Because of the lack of data for 50% strain values of the different sub-layers, a strain of 0.0005 was used for all iterations. The RQD value for each sub-layer was assumed to be the average of the upper and lower bound values. The strength reduction factors were obtained from the RQD values and the correlation proposed by Reese (1997).

The second step of curve fitting was performed to refine the curves obtained in the previous fitting process. In this step, only the strength reduction factors were varied. The fitted *p-y* curves for the upper, middle, and lower sub-layers of clayshale are presented in Figures 4, 5 and 6, respectively. The in-situ rock properties derived from the best-fit curves for each clayshale sub-layer are summarized in Table 3.

Using the best fitted theoretical *p-y* curves, the deflection profiles of caisson A were computed using Ensoft COM624 software. The computed deflection profiles were compared with the measured deflection profiles for different lateral load intensities. Hall (1999) documented the complete results of this analysis and comparison. Figures 7, 8 and 9 show the comparison for load intensities of 578, 1416 and 1573 kN (129, 316 and 351 kips), respectively. It is seen that the agreement between the two sets of data is not as good at the small load intensities. A possible explanation for the difference is that the collected field data under small loads may not be as accurate as those under larger loads.

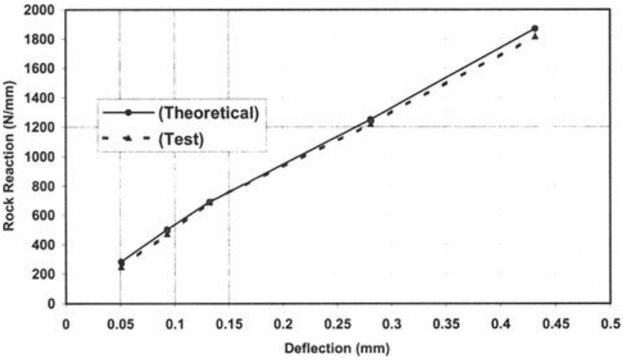

Figure 4. ***p-y*** **Curves for Upper Clayshale Sub-Layer**

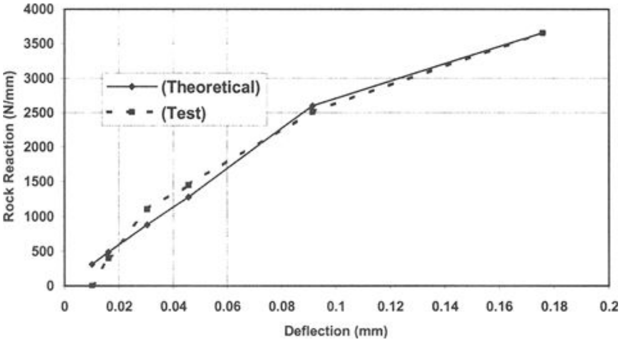

Figure 5. ***p-y*** **Curves for Middle Clayshale Sub-Layer**

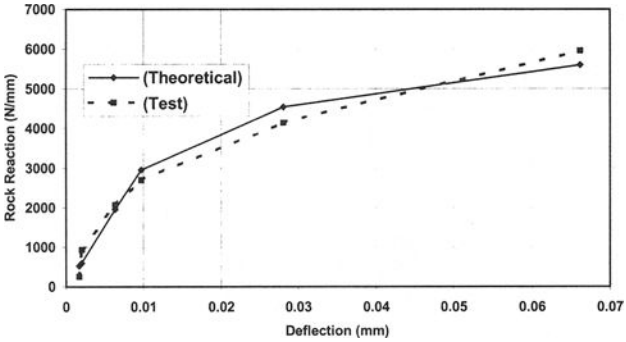

Figure 6. ***p-y*** **Curves for Lower Clayshale Sub-Layer**

Table 4. In-situ Rock Properties Determined from "Best Fit" Curves

	Strength Reduction Factor (α_r)	50% Strain (ε_{50})	E_{mass} (kPa/psi)	q_u (kPa/psi)
Upper Sub-layer	0.50	.0005	24,000/ 3500	4,134/600
Middle Sub-layer	0.46	.0005	120,000/17,000	5,512/800
Lower Sub-layer	0.39	.0005	1,200,000/170,000	13,000/1,850

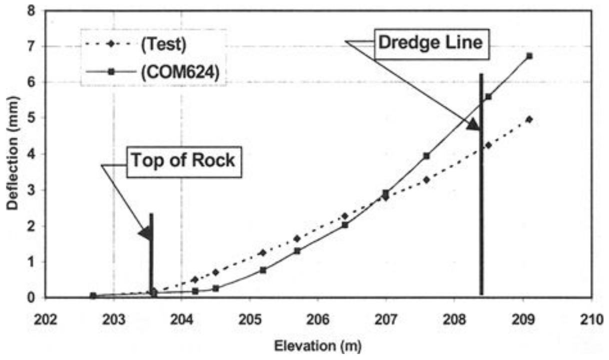

Figure 7. Comparison Between Predicted and Measured Deflection Profiles for 578 kN (129 kips) Lateral Load

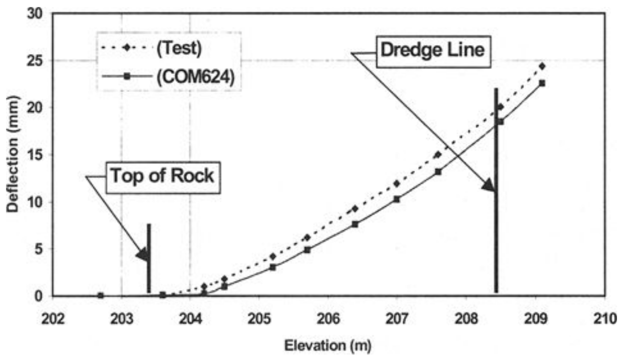

Figure 8. Comparision Between Predicted and Measured Deflection Profiles for 1,416 kN (316 kips) Lateral Load

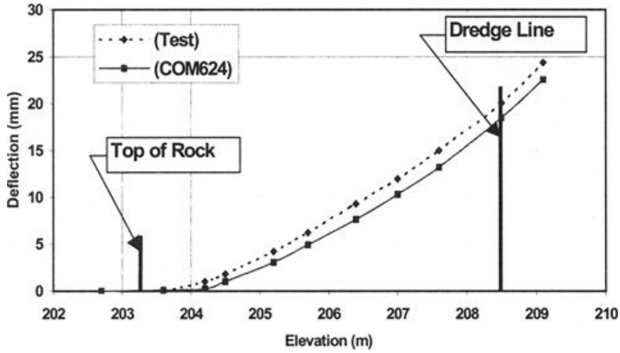

Figure 9. Comparison Between Predicted and Measured Deflection Profiles for 1,573 kN (351 kips) Lateral Load

Discussions

It is difficult to determine accurate in-situ rock properties for use in *p-y* curve analysis. The problem is further exacerbated when dealing with weak rock. The RMR correlation provides a range of values that are much more representative of the in-situ conditions in moderately weak to very weak rock, because the RMR correlation takes into account the effects of discontinuities on the overall behavior of the material much better than the RQD correlation. The condition and spacing of discontinuities have enormous impact on the rock mass elasticity and are vital to the accurate determination of rock mass behavior.

For high quality weak rock, the RQD correlation is an adequate means of determining the elastic modulus of the rock mass. Because materials having high RQD values are less fractured, discontinuities have much less influence on the in-situ properties of the material.

Based on the data analyzed, the strength reduction factor has little effect on the *p-y* curves for highly fractured very weak rock. For this type of material, it can be assumed that loading will cause little or no further fracturing. Thus, the elastic modulus becomes the governing parameter in the determination of *p-y* curves. Because of its highly fractured state, it is likely that very weak rock may be more accurately evaluated by using the methods already established for stiff granular materials. Further research is needed, however, to substantiate this postulation.

A higher strength intact material, similar to that found in the lower portion of the clayshale layer, is significantly affected by the load-induced fracturing. Based on the behavior of the clayshale investigated, a significant load-induced fracturing will likely occur only in the lower intact layers.

Using the iterative process discussed earlier, the strength reduction factor vs. RQD relationship was found to be different from that proposed by Reese (1997). The relationship for the clayshale layer investigated is not linear but displays a greater strength reduction between 0% and 45% RQD as shown in Figure 10. This is most likely due to the high degree of fracturing in the upper rock layer prior to loading.

A comparison between the measured and the analyzed deflection at the ground line, presented in Figure 11, demonstrates that although the discrepancy between the two sets of data is larger under smaller lateral loads, the overall agreement, generally speaking, is quite good. The poorer agreement under smaller lateral loads could be due to either inadequate input material properties in the computer analysis or less accurately measured deflection data, or both.

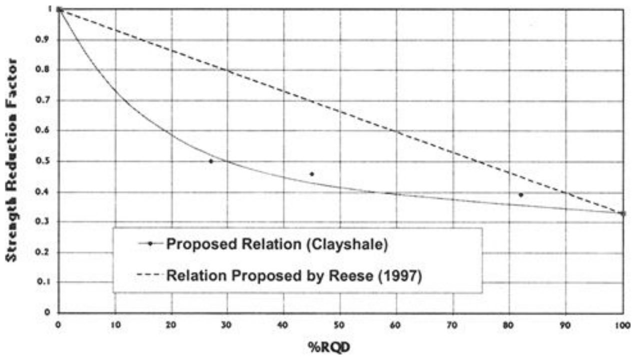

Figure 10. Proposed RQD vs. Strength Reduction Relationship

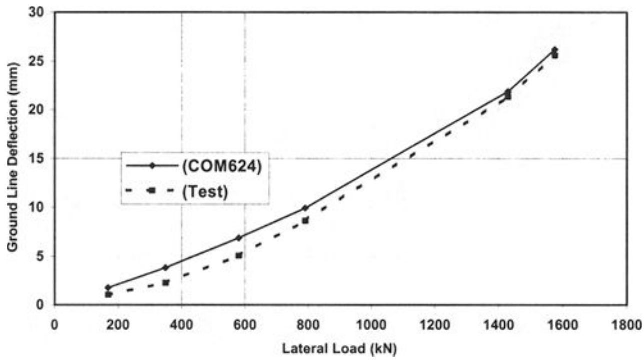

Figure 11. Comparison Between Predicted and Measured Ground Line Deflection